Talanta 100 (2012) 419–424

Contents lists available at SciVerse ScienceDirect

Talanta

journal homepage: www.elsevier.com/locate/talanta

A novel matrix additive, MCM-41-type mesoporous silica nanoparticles, used for analysis of peptides by MALDI-FT/ICRMS

Chen Jun [a,*,1], He Tianxi [b,c,1], Fan Xuemei [c]

[a] Beijing Institute of Microchemistry, No. 15 Xinjiangongmen Road, Beijing 100091, PR China
[b] Logistical Engineering University, Chongqing 400016, PR China
[c] Chemistry Department of Tsinghua University, Beijing 100081, PR China

ARTICLE INFO

Article history:
Received 6 April 2012
Received in revised form
7 August 2012
Accepted 9 August 2012
Available online 19 August 2012

Keywords:
Mesoporous silica nanoparticles
Peptide
Matrix-assisted laser desorption/ionization mass spectrometry
Matrix peak

ABSTRACT

Matrix-assisted laser desorption/ionization mass spectrometry (MALDI-MS) was thought to be unsuitable for the analysis of low-molecular-weight species since matrix peak noise made it difficult to identify analyte ions. In this study, MCM-41-type mesoporous silica nanoparticles (MSNs) were used as a matrix additive with saturated 2,5-dihydroxybenzoic acid (DHB) or α-cyano-4-hydroxycinnannic acid (CHCA) solution for the analysis of six peptides of a wide range molecular weight, Leu–Val, Phe–Val, Lue-Phe, bradykinin fragment 1–7, angiotensin II and ACTH fragment 18–39. It was shown that MSNs were capable of reducing matrix peaks with laser power lower than 34% of saturated DHB especially for low polarity analyte or CHCA especially for high polarity analyte with molecular weight less than 500 regardless of the analyte-to-matrix ratio. In addition, MSNs could suppress ionization of oligopeptide and polypeptide. The way MSN exerted its effect was supposed to be via attraction between surface silanol groups and the analyte.

1. Introduction

Matrix-assisted laser desorption/ionization mass spectrometry (MALDI-MS) method had been proved to be a powerful technique for mass spectrometric analysis of biomacromolecule, especially for peptides and proteins [1], accompanied with an idea that it was not suitable for the low-molecular-weight species ($MW < 500$), because the analyte ion was often subject to interference by the peaks of the matrix-related background noise in the low-mass region [2]. Proper analyte-to-matrix ratio was emphasized to reduce background noise [3]. Given that the concentrations of most analytes were probably unknown, from the application point of view, it seemed to be unfeasible to prepare the sample with an appropriate analyte-to-matrix ratio. To evade such flaw, matrix additives α-cyano-4-hydroxycinnannic acid (CHCA) [4], nitrilotriacetic acid [5] and 9-aminoacridine [6] had been added to restrict proton transmission or change its direction and reduce matrix background noise. Otherwise, inorganic nanoparticles [2] had been used for substitution in organic matrix to avert matrix peaks noise below 500 Da. In this case, surface modification or complex sample preparation was generally needed for metal nanomaterials, and an array of carbon cluster peaks often appeared in the low-mass region below m/z 300 at high laser power with carbon materials. Porous silicon was another one of the most used matrices for SALDI-MS (surface-assisted laser desorption/ionization mass spectrometry) because of its high absorption coefficients in the UV region. But it was easily oxidized when exposed to air for extended period which would affect the DIOS (desorption ionization from porous silicon) performance.

Regarding the drawbacks of porous silica, it may not be stable upon prolonged exposure to aqueous solutions and due to the variability of its pore size, its application to biomolecule adsorption and analysis was limited. Mesoporous materials had attracted much research attention due to their high surface area, tunable and uniform pore size and volume, and diversity in surface functionalization, which made them suitable as host materials to incorporate guest molecules [7]. Since the discovery of surfactant-templated synthesis of mesoporous silica materials in 1992 [8], many people explored the functionalization and utilization of these materials for various applications, such as catalysis, separation, sensors, imaging, enzyme immobilization and drug delivery [9,10]. It was suggested that moderate oxidation leads to the formation of acidic Si–OH groups that benefit the analyte ionization in DIOS-MS, whereas the formation of an overoxidized silicon oxide layer reduces the overall ionization efficiency [11]. Thus, the homogeneous 3 nm pore size of MCM-41-type MSNs with a certain Si–OH on its surface would be useful in testing molecules below 500 Da. Moreover, MSNs were believed to be more stable in aqueous solutions and air.

* Corresponding author. Tel.: +86 10 62887860 113; fax: +86 10 62781820.
E-mail address: chenjun05@tsinghua.org.cn (C. Jun).
[1] These authors contributed equally to this work.

0039-9140/$ - see front matter © 2012 Elsevier B.V. All rights reserved.
http://dx.doi.org/10.1016/j.talanta.2012.08.011

The original aspect of this work is that MSNs are firstly used as a matrix additive in MALDI-MS for analytes with molecular weight lower than 300 Da. Due to the difference of agent's size and charge, mesoporous nanoparticles were able to absorb protein and small bio-active molecules via aperture adjustment or surface modification [12]. In addition, the unique properties of nanomaterials greatly facilitate analyte desorption and ionization [13]. In this work, we made use of such character of MSNs in the application of peptide analysis by MALDI-FT-ICR/MS. Five peptides with a wide molecular weight range, Leu–Val (MW 230.3), Phe–Val (MW 264.3), bradykinin fragment 1–7 (MW 756.4), angiotensin II (MW 1045.5) and ACTH fragment 18–39 (MW 2464.2), were tested. The mechanism by which MSNs exerted their attraction was deduced by mass spectra of analytes with or without MSNs.

2. Experimental

2.1. Chemicals

Cetyltrimethylammonium bromide (CTAB, 99%) and tetraethyl orthosilicate (TEOS, 97%) were purchased from Sinopharm Chemical Reagent Co. Ltd. (China); 2,5-dihydroxybenzoic acid (DHB, matrix for MALDI-TOF/MS) was purchased from TCI-EP (Japan); Leu–Val (desiccate), Phe–Val (desiccated), Leu–Phe (desiccated), bradykinin fragment 1–7 (10 μmol/L), angiotensin II (10 μmol/L), ACTH fragment 18–39 (10 μmol/L) and α-cyano-4-hydroxycinnannic acid (CHCA, matrix for MALDI-TOF/MS) were purchased from Sigma-Aldirich (US); acetonitrile (HPLC grade) was purchased from CNW (USA). DI water was generated by a Milli-Q Integral 3 A10 system.

Individual stock aqua solutions (0.01 g/mL) of Phe–Val and Leu–Val were stored at −20 °C; the DHB stock solution (0.15 g/mL) was prepared in 1 mL acetonitrile: 0.1% TFA 1:1 (v:v) and stored at 4 °C; the CHCA stock solution (0.01 g/mL) was prepared in 1 mL acetonitrile: 0.1% TFA 4:1 (v:v) and stored at 4 °C; 0.05 g of MSNs was suspended in 4 mL water–acetonitrile (1:1, v:v) by vortexing for 1 min [2].

2.2. Synthesis of MCM-41-type mesoporous silica nanoparticles (MSNs)

MSNs were synthesized following the reported procedure with slight modification [14]. In brief, 2 M NaOH solution (7.0 mL) was added to 720 mL aqueous solution of CTAB (2 g). At 80 °C, TEOS (15 mL) was added dropwise at a rate of 1 mL/min. The mixture was stirred at 80 °C for 2 h. Finally the precipitate was filtered, rinsed with MeOH, and was dried at 60 °C. To prepare the final MSNs, the as-synthesized solid was calcined at 550 °C for 5 h in order to remove CTAB.

2.3. Sample preparation

Each peptide was mixed with equivalent volume of DHB solution and divided into two parts. One part (A) was reserved; equivalent volume of MSNs suspension was added to the other part (B) and mixed thoroughly. The dry-drop method was used to spot 1 μL (A) and 2 μL (B, suspension) to the stainless steel well, and then dried in air. Five plots of each sample were prepared in this work.

2.4. FT-ICR/MS parameter

All mass spectra data was acquired by a MALDI-FTMS (920, Varian, USA) equipped with an orion air-cooled Nd:YAG laser (532, 355, and 266 nm). Single collection was performed after five times lasing. The *m/z* scan range of Leu–Val and Phe–Val was 150–500, and 500–3000 for the other three peptides in positive mode. 512 K was chosen for the number of samples, and the transient length was calculated automatically by Omega (9.0 beta, Varian).

2.5. N_2 adsorption

N_2 sorption isotherms were obtained at 77 K on a Tristar II 3020 automated sorption analyzer (Micromeritics Instrument, USA). The sample was out-gassed at 90 °C for 10 h before the measurements. The surface area was determined using the Brunauer–Emmett–Teller (BET) method. The average mesopore size was obtained from the maximum of the pore size distribution calculated from the adsorption branch of the isotherm by means of the Barrett–Joyner–Halenda (BJH) method. The measured BET surface area of the MSNs was 1029 m^2/g. The corresponding BJH average pore size of the MSNs was 3.150 nm and the pore volume was 0.9689 cm^3/g (Table 1).

3. Results and discussions

3.1. MSNs deduced matrix background noise for dipeptide analysis

There was no peak detected when MSNs were used as a matrix. Thus, it was used with DHB as a matrix additive. DHB was the most used matrix in the MALDI-MS analysis; *m/z* 187, 217, 245, and 273 were the main peaks of matrix background noise when DHB was used. For samples without MSNs, when laser energy was 30%, the sodium ion adduct $[M+Na]^+$ (287.2) of Phe–Val could be hardly detected with abundant matrix peaks (Fig. 1A) while the sodium ion adduct $[M+Na]^+$ (253.2) of Leu–Val was not found (Fig. 2A); when laser energy was 33% (data not shown), the intensity of $[M+Na]^+$ (287.2) reached 70% of base peak at *m/z* 245, and $[M+Na]^+$ (253.2) was hardly detected (Fig. 2C); $[M+Na]^+$ (287.2) became the base peak when laser energy reached to 39% with matrix (Fig. 1C), but the spectra became complex when laser power was over 40% (Fig. 1E), but $[M+Na]^+$ (253.2) was still lower than 40% of matrix peak.

Regarding Phe–Val with MSNs, nearly no ions were detected with laser power lower than 31%; $[M+Na]^+$ (287.2) became the base peak with 32–33% laser power while the intensities of matrix peaks 273 and 245 were lower than 5% of that of the base peak (Fig. 1B); with laser power higher than 34%, matrix peak became the base peak (Fig. 1D). The intensity of $[M+Na]^+$ (287.2) decreased with the increase in laser power, and it was only 10% of matrix base peak when laser power reached 40% (Fig. 1F). Regarding Leu–Val with MSNs, when laser power was 30%, $[M+Na]^+$ (253.2) was the base peak with low intensity, $[M-H+2Na]^+$ (275.2) was the secondary base peak, and no other matrix peaks were found (Fig. 2B). No analyte ions were detected but matrix peaks were found without MSNs when laser power was 30% (Fig. 2A). The intensity of both $[M+Na]^+$ (253.2) and $[M-H+2Na]^+$ (275.2) increased with 33% laser power; meanwhile, matrix peaks increased to approximately 20% of base peak

Table 1
BET and BJH parameters of MSNs.

Material	BET surface area-to-volume ratio (m^2/g)	[a]BJH pore volume (cm^3/g)	[b]BJH pore size (nm)
MSNs	1029	0.9689	3.150

[a] BJH pore volume.
[b] BJH pore size was the mean value calculated by adsorption curve with the BJH method.

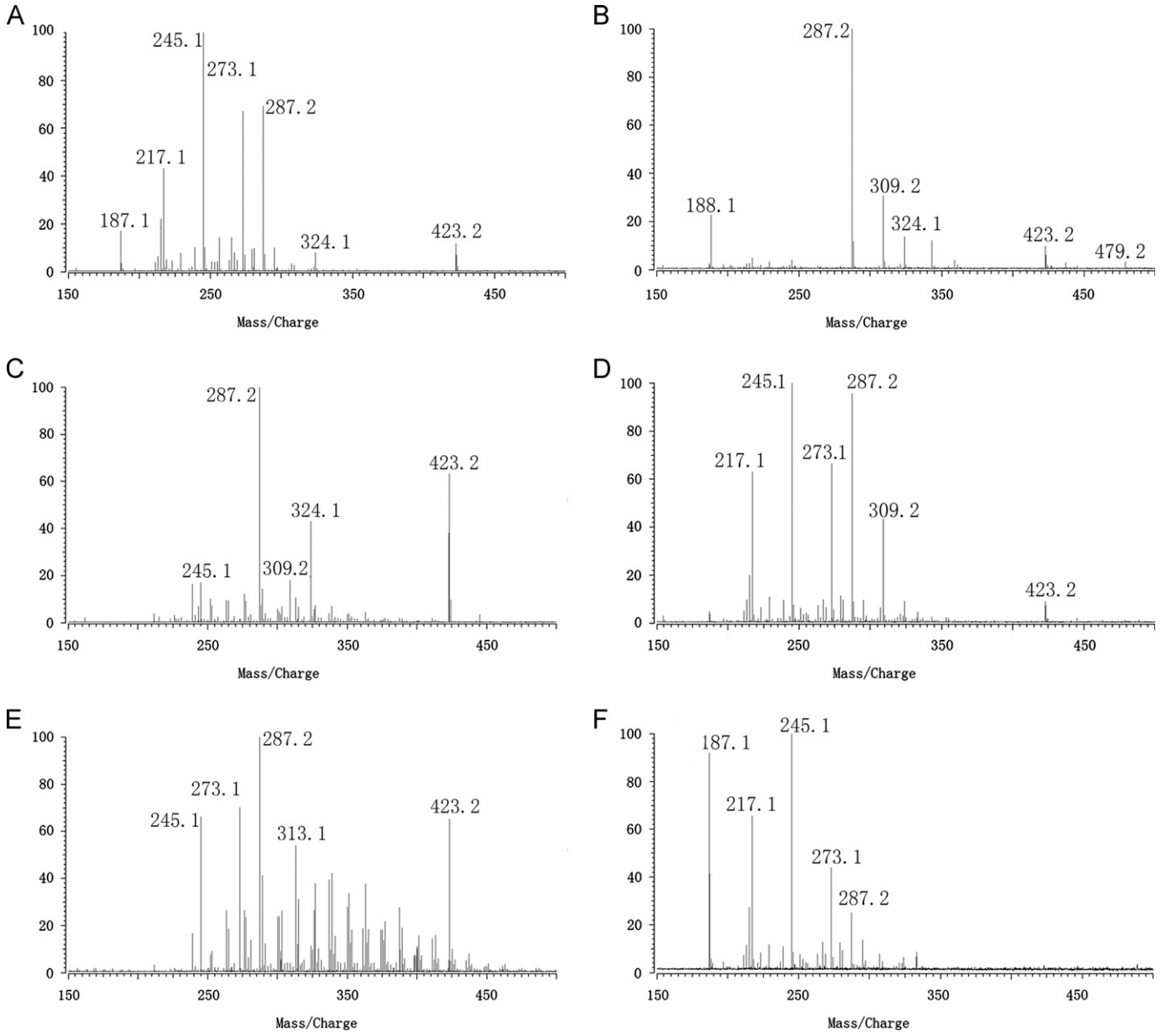

Fig. 1. Mass spectra of Phe–Val with and without MSNs at different laser powers. (A), Phe–Val at 30% laser power; (B), Phe–Val with MSNs at 33% laser power; (C), Phe–Val at 39% laser power; (D), Phe–Val with MSNs at 35% laser power; (E), Phe–Val at 40% laser power; (F), Phe–Val with MSNs at 39% laser power.

(Fig. 2D). However, $[M+Na]^+$ (253.1) was only 20% of matrix base peak 273.1 (Fig. 2C).

These results showed that the intensity of dipeptide and matrix ion could be increased by laser power enhancement, but the relative intensity of analyte to matrix peaks was related to its chemical structure. When laser power was 30%, Phe–Val was detected but Leu–Val was not found. When laser power was 39%, the sodium adduct ion $[M+Na]^+$(287.2) of Phe–Val was found to be the base peak; however, the sodium adduct ion $[M+Na]^+$ (253.2) of Leu–Val was still less than 40% of matrix base peak. There were probably two reasons for such phenomena: one was that the benzene ring in Phe–Val facilitated ionization by making it easy to absorb laser energy with no MSNs, and the other was that the interaction of Leu–Val and MSNs was larger since its molecular diameter was larger than that of Phe–Val; thus the desorption of Leu–Val needed more energy compared to Phe–Val.

With MSNs at low laser power, matrix peaks were not found in spectra whereas their base peak was the alkalis adducted analyte ion, but matrix ions appeared to be the base peak with MSNs at higher laser power. The laser-induced rapid temperature increase in the LDI substrate was believed to be the most important factor that had been widely attributed to the thermal desorption of analyte molecules without thermal decomposition in SALDI-MS [15]. The low thermal conductivity of mesoporous silica nanoparticles could increase the peak temperature by confining the heat near the surface. Therefore, the use of DHB with mesoporous silica nanoparticles results in a remarkable decrease in the minimum laser irradiation energy required for analyte desorption. In addition, there were silanol groups at the MSNs inner-surface which could interact with hydrophilic groups and components. Since the polarity of matrix DHB was stronger than those of Phe–Val and Leu–Val, the interaction of DHB with MSNs surface was certainly the strongest. As the interaction of DHB and MSNs was believed to be due to hydrogen bond and Van der Waals' force, DHB could be desorbed from MSNs if enough energy was afforded. Therefore, matrix peaks disappeared at low laser power while analyte peaks were found, but

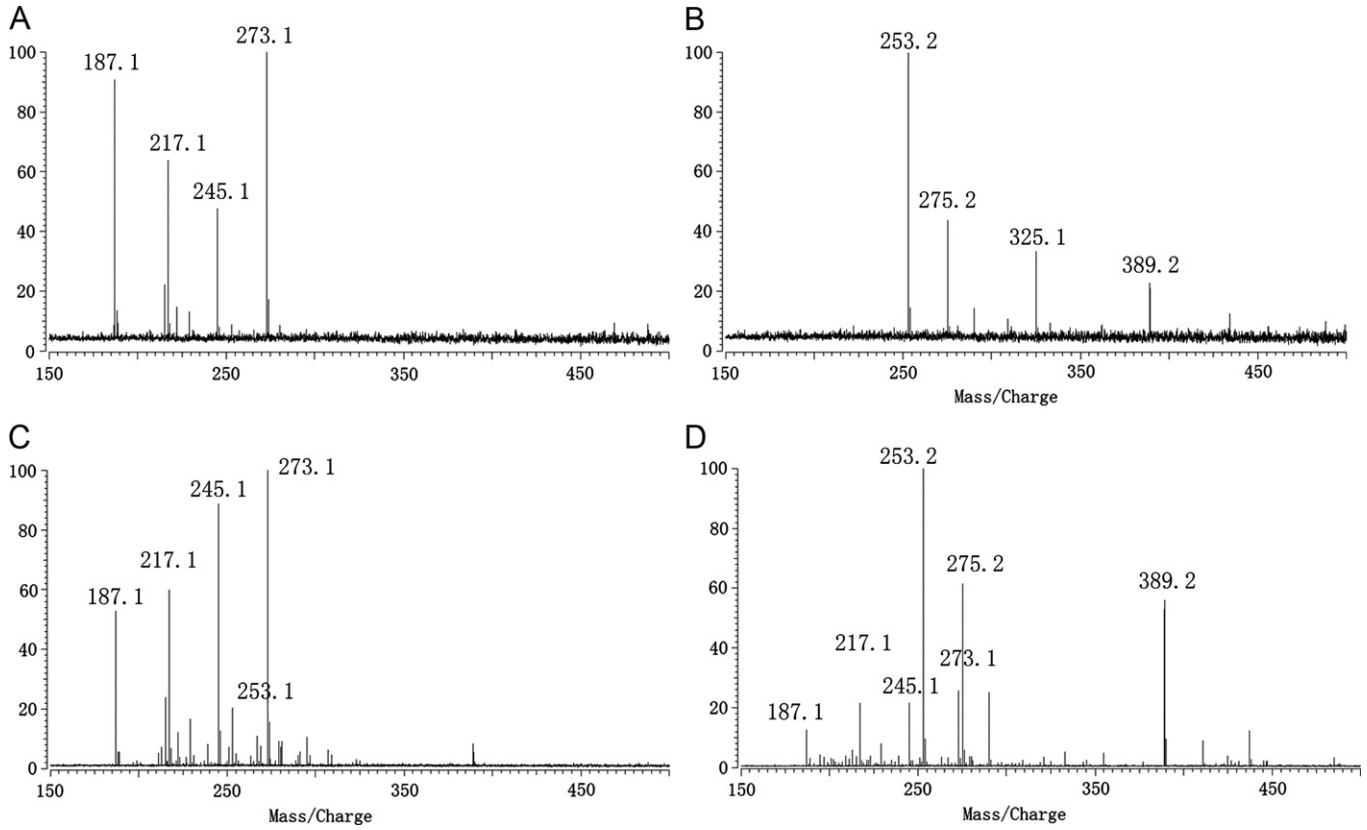

Fig. 2. Mass spectra of Leu–Val with and without MSNs at different laser powers. (A), Leu–Val at 30% laser power; (B), Leu–Val with MSNs at 30% laser power; (C), Leu–Val at 33% laser power; (D), Leu–Val with MSNs at 33% laser power.

accompanied with enhanced laser power. In this study, 30–32% laser power seemed to be optimal for dipeptide's analysis with MSNs.

Nearly the same results were obtained when CHCA was used as a matrix substitute for DHB. Only matrix background of CHCA was found with 33% laser power in the mass spectra of Leu–Val without MSNs (Fig. 3A), but $[M-H+2Na]^+$ (275.2) was clearly the base peak with low matrix background when MSNs were added (Fig. 3B). The interaction of MSNs and CHCA could be deduced from the fact that when Phe–Val was analyzed with 33% laser power, $[M+CHCA+Na]^+$ (476.2) was found to be the base peak without MSNs (Fig. 3C), and $[M-H+2Na]^+$ (309.2) was obtained but no 476.2 peak when MSNs were added (Fig. 3D).

3.2. DHB or CHCA matrix background noise for Leu–Phe with MSNs

When CHCA was used as a matrix for MALDI-MS analysis of Leu–Phe, no difference was found between with or without MSNs but only CHCA matrix peaks were obtained (Fig. 4A and B). This fact suggested that CHCA might not be suitable for the MALDI analysis of Leu–Phe. Both $[M+H]^+$ (279.1) and $[M+Na]^+$ (301.2) of Leu–Phe with abundant matrix peaks had been obtained when DHB was used as a matrix without MSNs (Fig. 4C), but $[M+Na-H_2O]^+$ (283.2) was obtained as the base peak with no matrix peaks when MSNs were added (Fig. 4D). The reason for such phenomenon was probably the structure difference between DHB and CHCA causing, the interaction of DHB and MSNs to be powerful.

3.3. MSNs suppressed ionization of oligopeptide and polypeptide

For analysis of oligopeptides, bradykinin fragment 1–7 (MW= 756.3) and angiotensin II (MW=1045.5), and the polypeptide ACTH fragment 18–39 (MW=2464.2) the matrix peaks were not detected as they were mainly below 300 amu whereas the coil we chose for these three peptides was suitable for the detection of ion with m/z above 500. Thus, matrix suppression was not needed for great-molecular-weight species (MW > 500).

Oligopeptides and polypeptides could be detected without MSNs at 32% laser power, whereas they could not be found with MSNs even at 40% laser power. When laser power was higher than 40%, the molecular ions of these three peptides still could not be found, but fragment ions emerged especially for the polypeptides. It was deduced from these results that MSNs could suppress desorption of oligopeptides and polypeptides with MW > 750.

Via calculated simulation, although the molecular size of ACTH fragment 18–39 was almost 3 nm which was the mean pore size of MSNs, the sizes of both bradykinin fragment 1–7 and angiotensin II were far less than 3 nm. Fragment ions without molecular ions appeared, indicating that MSNs did not bind the energy transition from matrix to analyte. What is more, the disappearance of molecular ions of oligopeptides with MSNs showed that the suppression of peptide desorption was not just filtration since it was much smaller than MSNs pore size and the adsorption mechanism which had been discussed in dipeptide's analysis seemed to be essential. With the peptide chain extended, the polarity also increased. In addition, the polarity groups of peptide were prone to be external in aqua solution (Fig. 1), which enhanced interaction with Si–OH existing on MSNs surface. Given that the energy needed to break off such interaction was higher than what was needed to fragment molecules, fragment ions were found without molecular ions when laser power was high enough.

3.4. Optimized MSNs concentration

MSNs with different concentrations were prepared by suspending 0.01, 0.02, 0.03, 0.04, 0.05, 0.06, 0.07, 0.08, 0.09, and 0.1 g in 4 mL water–acetonitrile (1:1, v:v). No significant difference in

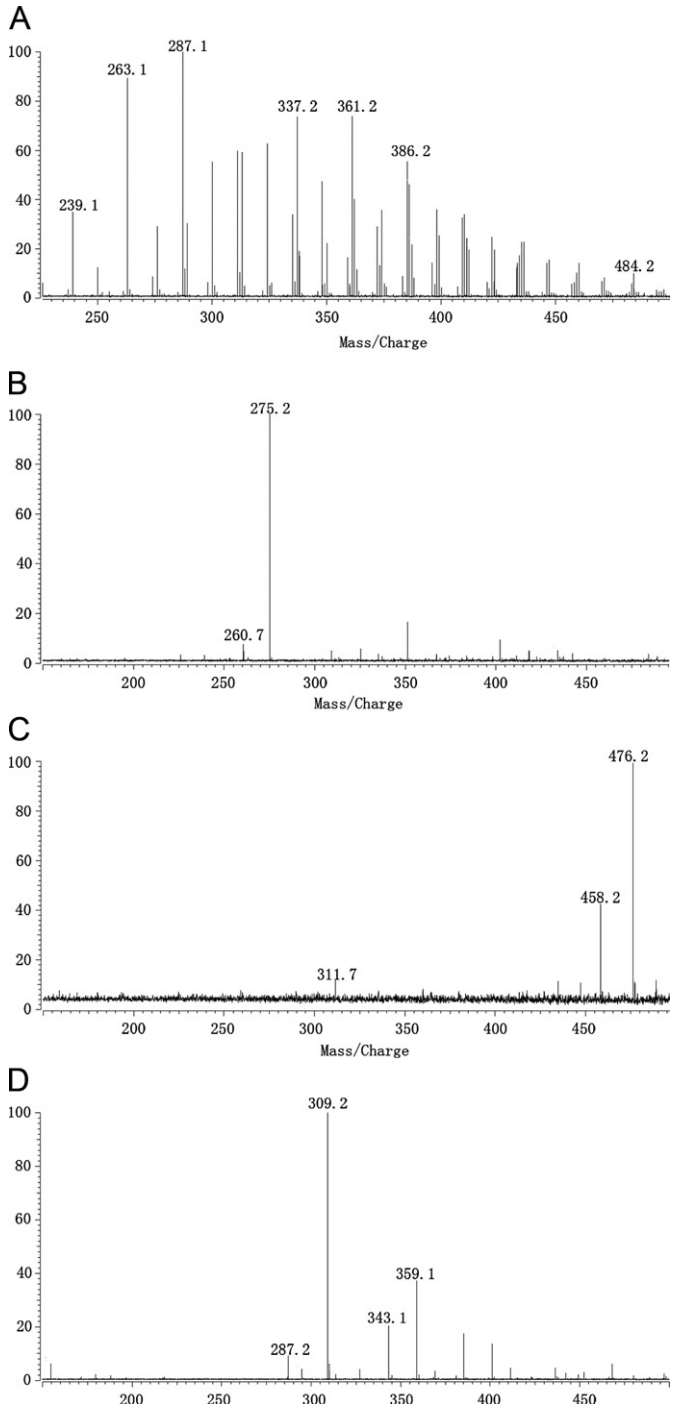

Fig. 3. Mass spectra of Leu–Val and Phe–Val using CHCA as a matrix at 33% laser power. (A), Leu–Val without MSNs; (B), Leu–Val with MSNs; (C), Phe–Val without MSNs; (D), Phe–Val with MSNs.

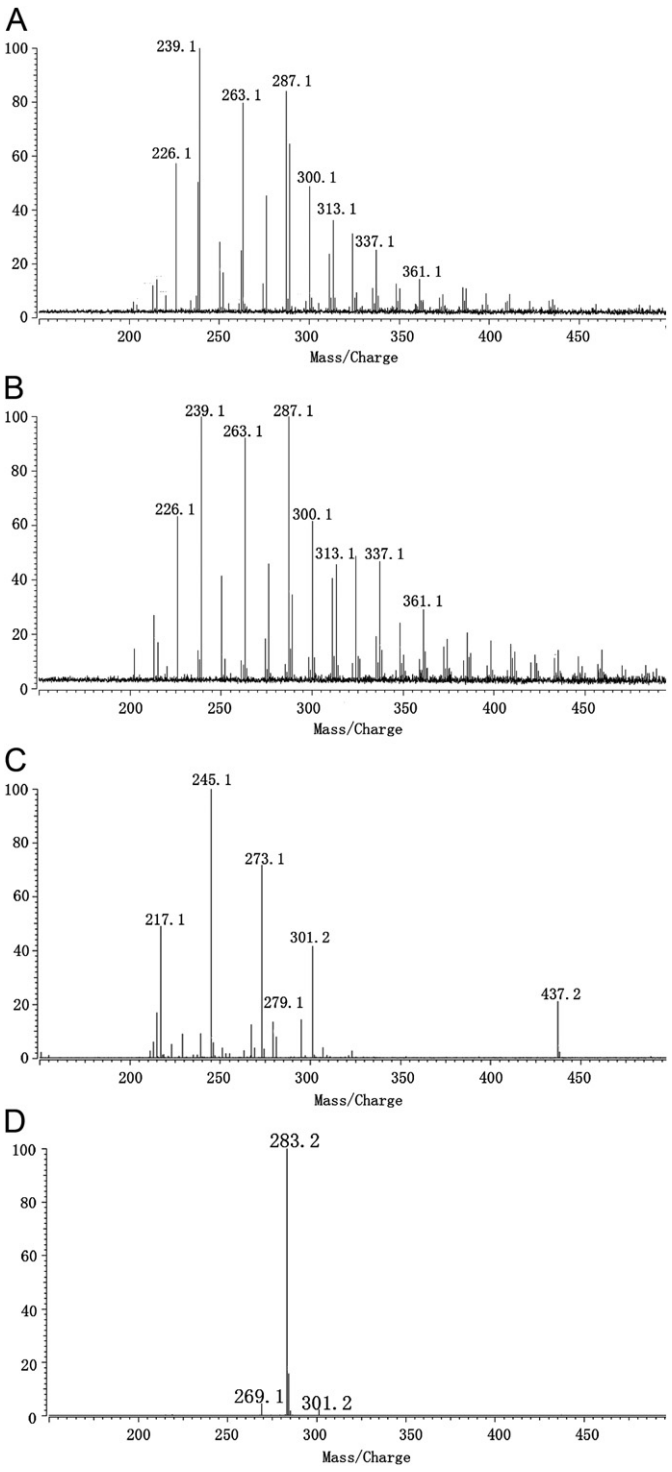

Fig. 4. Mass spectra of Leu–Phe using CHCA or DHB as a matrix at 33% laser power. (A), CHCA without MSNs; (B), CHCA with MSNs; (C), DHB without MSNs; (D), DHB with MSNs.

mass spectra was found compared to peptides without MSNs when the concentration of MSNs was lower than 0.03 g/4 mL. When it was higher than 0.08 g/4 mL, after drying up, MSNs were too dense for analyte ions to be detected. Thus, 0.05 g/4 mL was chosen as the optimized concentration in the recent work. Matrix peak suppression using MSNs as matrix adductive resulted in improved detection sensitivity for all these three dipeptides from 50 μg/mL to nearly 80 ng/mL. Although MALDI-MS is not suggested as a quantitative method, the low detection limit would be helpful for qualitative analysis especially combined with high resolving mass apparatus such as FT-ICR/MS.

4. Conclusions

In this study, we used MCM-41-type MSNs as a matrix additive of DHB for MALDI-MS analysis of peptides, Leu–Val, Phe–Val, Leu–Phe, bradykinin fragment 1–7, angiotensin II and ACTH fragment 18–39. MSNs could not be used as a matrix due to the fact that no ion was found with MSNs only. With MSNs as a matrix additive, saturated DHB aqueous solution could be used as the need was to confirm only appropriate laser power but not analyte-to-matrix ratio to reduce

matrix ions. The way MSNs exerted their impact on peptide analysis was probably by laser-induced rapid temperature increase and interaction of analyte and Si–OH existing on the MSNs surface. For dipeptide's analysis, DHB matrix peak reduced FTMS spectra could be obtained at low laser power with MSNs, whereas for analysis of oligopeptides and polypeptides, molecular ions were not found since the interaction of MSNs and analyte was too strong to let analyte desorb at laser power was below 40%. As the coil chosen for low-molecular-weight species was suitable for the mass/charge range of 150–500, DHB coupled with MSNs could be useful for the detection of molecule below 500 Da with simple sample preparation.

References

[1] L.L. Sun, Q. Zhao, G.J. Zhu, Y. Zhou, T.T. Wang, Y.C. Shan, K.G. Yang, Z. Liang, L.H. Zhang, Y.K. Zhang, Rapid Commun. Mass Spectrom. 25 (2011) 1257–1265.
[2] T. Kinumi, T. Saisu, M. Takayama, H. Niwa, J. Mass Spectrom. 35 (2000) 417–422.
[3] R. Knochenmuss, V. Karbach, U. Wiesli, K. Breuker, R. Zenobi, Rapid Commun. Mass Spectrom. 12 (1998) 529–534.
[4] I.P. Smimov, X. Zhu, T. Taylor, Y. Huang, P. Ross, I.A. Papayanopoulos, S.A. Martin, D.J. Pappin, Anal. Chem. 76 (2004) 2958–2965.
[5] J.S. Kim, J.Y. Kim, H.J. Kim, Anal. Chem. 7 (2005) 7483–7488.
[6] Z. Guo, L. He, Anal. Bioanal. Chem. 387 (2007) 1939–1944.
[7] F. Hoffmann, M. Cornelius, J. Morell, M. Froba, Angew. Chem. Int. Ed. 45 (2006) 3216–3251.
[8] C.T. Kresge, M.E. Leonowice, W.J. Roth, J.C. Vartuli, J.S. Beck, Nature 359 (1992) 710–712.
[9] S.B. Wang, Micropor. Mesopor. Mater. 117 (2009) 1–9.
[10] H. Kim, S. Kim, C. Park, H. Lee, H.J. Park, C. Kim., Adv. Mater. 22 (2010) 4280–4283.
[11] Q. Liu, L. He, J. Am. Soc. Mass Spectrom. 19 (2008) 8–13.
[12] Y.X. Qi, J.Y. Wei, H. Wang, Y.J. Zhang, J. Xu, X.H. Qian, Y.F. Guan, Talanta 80 (2009) 703–709.
[13] K.P. Law, J.R. Larkin, Anal. Bioanal. Chem. 399 (2011) 2597–2622.
[14] R. Liu, X. Zhao, T. Wu, P.Y. Feng, J. Am. Chem. Soc. 130 (2008) 14418 11419.
[15] T. Yonezawa, H. Kawasaki, A. Tarui, T. Watanabe, R. Arakawa, T. Shimada, F. Mafune, Anal. Sci. 25 (2009) 339–346.